Configurational disorder and magnetism in double perovskites: A Monte Carlo simulation study

Carlos Frontera and Josep Fontcuberta
Institut de Ciència de Materials de Barcelona, CSIC, Campus Universitari de Bellaterra, E-08193 Bellaterra, Spain
(Received 26 June 2003; revised manuscript received 19 September 2003; published 9 January 2004)

We examine the effect of antisite disorder on the magnetic properties of Sr_2FeMoO_6 by means of Monte Carlo simulation of a physically reasonable model that takes into account the origin of the ferromagnetic interactions between Fe ions. With this model, the main experimental features found in these compounds are recovered by the simulations. Special attention has been paid to the study of the critical properties as a function of disorder. The critical exponents β and γ calculated from the simulations are consistent with experiment.

DOI: 10.1103/PhysRevB.69.014406 PACS number(s): 75.30.Kz, 75.47.−m, 75.10.Hk, 05.50.+q

I. INTRODUCTION

Double perovskites of the type A_2FeMO_6 (where A=Ca, Sr, Ba and M=Mo, W, Re) have been intensively studied during recent years. Some families of these compounds present considerable low-field magnetoresistance and a half-metallic character. These properties, together with their Curie temperature (T_C), which is usually well above room temperature,[1] make these compounds very promising candidates for spintronics and other applications. It has been proposed that the origin of the magnetic interaction stabilizing the ferromagnetic (FM) order relies on the antiferromagnetic (AFM) interaction between itinerant t_{2g}-spin down electrons of the conduction band and the localized magnetic moment of Fe ions.[2] This conduction band is formed, for instance in the case of Sr_2FeMoO_6, by hybridized Mo ($4d$) and Fe ($3d$) orbitals and is responsible of the metallicity of this compound. In fact, only when the contribution coming from these delocalized electrons is taken into account, it is possible to explain the magnetic properties of Sr_2FeMoO_6 above T_C.[3] It is thus believed that the FM interaction between Fe ions is transmitted by itinerant t_{2g}-spin down electrons with an active participation of Mo orbitals.

From an ionic point of view, Fe and Mo in Sr_2FeMoO_6 can present two different valence distributions: Fe^{3+}/Mo^{5+} ($3d^5$-$4d^1$) and Fe^{2+}/Mo^{6+} ($3d^6$-$4d^0$). Different experimental techniques provide different answers to the question of which valence distribution is stabilized in this compound. By means of neutron powder diffraction a very small magnetic moment has been found in the Mo site (ranging between $0\mu_B$ and $0.3\mu_B$),[4–7] which would favor the Fe^{2+}/Mo^{6+} valence distribution. In contrast, Mösbauer spectroscopy indicates that the valence of Fe is closer to 3+ than to 2+.[8,9] However, the fact that a certain fraction of the electrons are delocalized can make the ionic picture mentioned not accurate enough to describe this system.

In the ideal double perovskite Fe and Mo ions, placed in the A position of the perovskite structure, are ordered forming two interpenetrated cubic lattices. In real compounds, there is a certain number of misplaced cations or antisites (AS) consisting in Fe (Mo) positions occupied by Mo (Fe) ions. The concentration of AS strongly depends on the synthesis (or crystal growth) conditions and affects not only the transport and magnetoresistance properties of the samples but also the magnetic properties.[10] It has been experimentally found that the presence of AS reduces the low-temperature saturation magnetization and widens the magnetic transition.[11] As the concentration of AS grows, the peak of the measured magnetic susceptibility shrinks, thus suggesting that the divergence of the correlation length is changed by some kind of local magnetism confined in finite domains.[12] Interestingly, at large enough AS concentration, the Arrot's plots of $M(H)$ curves reveal a loss of criticality.[11] Similar behavior has been predicted by the random-field Ising model.[13] However, it is not clear that the Ising model, with a symmetry-breaking random field, would have the same physics as a system with random AS disorder.

The effect of AS has been previously studied by means of Monte Carlo simulations by Ogale *et al.*[14] using an Ising model in which only exchange Fe-Fe and Fe-Mo nearest neighbor (n.n.) AFM interactions are considered. In that work some of the features induced by AS are recovered, but the criticality of the transition and its dependence on AS concentration were not deeply studied. In this paper we first introduce a different model that tries to explicitly include the origin of the FM Fe-Fe interactions. These interactions are mediated by spin-down Fe(t_{2g}) electrons delocalized in a conduction band that is formed by Mo orbitals. So, these electrons need the presence of Mo ions to effectively induce a FM Fe-Fe interaction. The introduction of AS locally suppresses this interaction, thus modifying the magnetic properties of these compounds. In this sense, the main motivation of the present work is to study, within this more physically reasonable context, the effect of AS disorder in order to understand the origin of the experimental observations. It is of special interest to study the criticality of this system as a function of disorder and to determine if a large amount of AS can induce a loss of criticality.

II. MODEL AND MONTE CARLO SIMULATION DETAILS

A. Model

As we are interested in studying the effect of disorder in the magnetic behavior, we have used a lattice model in which only the magnetic ions (Fe and Mo) are taken into account. These ions are considered to be placed on the corners of a cubic lattice of $N=L\times L\times L$ sites. In real systems there is a slight deviation from this assumption but the differences in the Mo-Fe distances in the three directions are small (about 0.2%).[15] In addition, we assume that the magnetic moment

comes exclusively from Fe ions and that the role of Mo ions is to transmit the FM interaction. As mentioned, this is justified by the fact that neutron-diffraction results show a small magnetic moment in Mo ions ($M_{\mathrm{Mo}} \leqslant 0.3\mu_B$).[4–7] Therefore the Fe-Mo exchange interaction must be less important than the magnetic interaction transmitted by itinerant electrons and it is thus reflected in the model. In order to reproduce the value of the saturation magnetization we take $S=2$ for Fe ions. This model can be viewed as corresponding to valences distribution $\mathrm{Mo}^{6+}/\mathrm{Fe}^{2+}$ ($4d^0/3d^6$).

In order to implement the model, we define two variables at each lattice site. The first one, x_i, takes the value 0 if the ith site is occupied by a Mo ion and 1 if it is occupied by a Fe ion. The second one, S_i, is defined at the sites where $x_i=1$ and it is the value of the third component of the spin S_z at ith position, where z is the direction of the external magnetic field. It can take the values $S_i=-2,-1,0,1,2$. The Hamiltonian used has two terms. One accounts for the strong AFM exchange interaction between Fe ions in n.n. positions. The other one tries to mimic the effective FM interaction introduced by the itinerant electrons of the conduction band. To model this term we assume that the delocalized electrons of a Mo ion extend up to the Fe in its n.n. positions, thus introducing an effective FM coupling between these Fe ions. So, the Hamiltonian reads

$$\mathcal{H}_{\{x_i\}}(\{S_i\}) = -J_{FM}\sum_{i,j,k} x_i S_i (1-x_j) x_k S_k + J_{AFM}\sum_{i,j}^{\text{n.n.}} x_i S_i x_j S_j - H\sum_{i=1}^{N} x_i S_i , \qquad (1)$$

where J_{FM} is the FM (mediated by itinerant e_g electrons) interaction, J_{AFM} is the AFM (exchange) Fe-Fe interaction, and H is the external magnetic field (which will be taken as zero along the paper). The first sum extends over all i,j,k positions such that i,j and j,k are n.n. pairs and $i \neq k$. The terms inside the sum are nonvanishing when j site is occupied by a Mo ion and i and k sites by Fe ions. This term introduces FM interactions between Fe in second (next n.n., n.n.n.) and third coordination spheres. It is worth noting that, in contrast with simulations previously reported,[14] the strength of the FM interaction between Fe ions in a n.n.n. position depends on the atoms surrounding those ions. It can take the values zero, J_{FM}, or $2J_{FM}$ (see Fig. 1). The sum in the second term extends over all n.n. pairs in the lattice and accounts for the AFM Fe-Fe (n.n.) exchange interaction.

We have chosen the value of $J_{FM}=7.79K\,k_B(g\mu_B)^{-2}$ ($k_B \equiv$ Boltzmann's constant; $g=2$; $\mu_B \equiv$ Bohr's magneton) that reproduces a Curie temperature $T_C \approx 420$ K for an antisite defects free (AS=0) system with $L=40$. The value taken for $J_{AFM}=52.8K\,k_B(g\mu_B)^{-2}$ has been chosen to reproduce the value of $T_N \approx 750$ K found for $LaFeO_3$ with the same system size.

B. Monte Carlo simulation details

The first step to perform the simulations consists in designing the AS positions (quenched disorder). With this purpose, we first define a perfectly ordered lattice where all the Fe ($x_i=1$) ions are surrounded by six Mo ($x_i=0$) ions. Next, we randomly choose the appropriate fraction of Fe and Mo sites to interchange them. Each realization of the quenched disorder ($\{x_i\}$ set) defines a different Hamiltonian following Eq. (1).

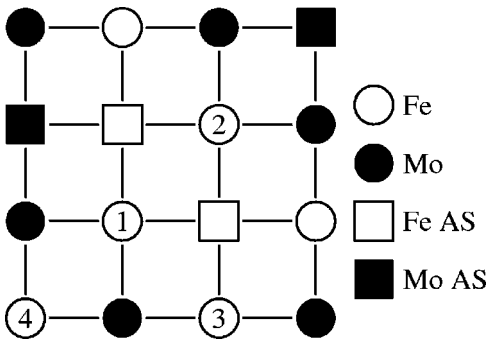

FIG. 1. Schematic representation of possible FM interaction strengths. The model used introduces FM coupling between Fe in the third coordination sphere, for instance, between iron labeled as "3" and "4." The strength of FM interaction in n.n.n. positions depends on the local configuration and it can take the values 0 (e.g., between "1" and "2"), J_{FM} (e.g., between "1" and "3"), and $2J_{FM}$ (e.g., between "1" and "4").

Monte Carlo simulations have been performed using Glauber dynamics and "heat bath" algorithm. We sequentially run along all Fe ions, for each we change the value of S_i to a new value $S_i'=-2,-1,0,1,2$ randomly chosen with probability

$$P(S_i') = \frac{\exp\{-\mathcal{H}_{\{x_i\}}(S_1,S_2,\ldots,S_i',\ldots,S_N)/(k_BT)\}}{\sum_{S_i=-2}^{2}\exp\{-\mathcal{H}_{\{x_i\}}(S_1,S_2,\ldots,S_i,\ldots,S_N)/(k_BT)\}} . \qquad (2)$$

We define one Monte Carlo step (MCS) as a run through all Fe ions. In order to analyze finite-size effects, simulations have been performed on lattices of size ranging from $L=10$ ($N=10^3$ spins) to $L=80$ ($N=512\times10^3$ spins), with periodic boundary conditions. Simulations have been done starting from the lowest temperature of each run. Initially, for this lowest temperature, all the Fe ions at the right positions take $S_i=2$ whereas those occupying AS positions take $S_i=-2$. A number of MCS's (ranging between 1000 and 2000) are performed to reach thermal equilibrium. Thermal averages of the physical magnitudes are obtained by averaging over a long time (about 3000 MCS's after thermalizing). For subsequent temperatures, the last configuration of the previous temperature is taken as initial configuration. All the results have been averaged over different realizations of the configurational disorder ranging from 100 (for the smallest system sizes) to 20 for $L=80$. By using this procedure, we obtain the thermal averages: $\langle M\rangle$, $\langle|M|\rangle$, $\langle M^2\rangle$, and $\langle M^4\rangle$. From those averages we calculate the magnetic susceptibility and the fourth-order Binder's cumulant:

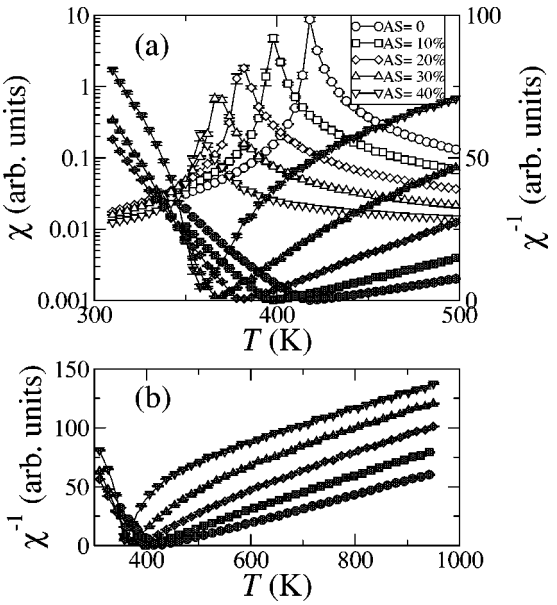

FIG. 2. (a) Temperature dependence of the magnetic susceptibility (open symbols; left axis) and its inverse (filled symbols; right axis) for system size $L=40$ with different amount of AS as labeled. Data correspond to the average of 40 realizations of disorder. (b) Inverse of the susceptibility up to high temperature in the same cases.

$$\chi \equiv \left(\frac{\partial \langle M \rangle}{\partial H} \right)_T = \frac{1}{T} \frac{1}{N} (\langle M^2 \rangle - \langle M \rangle^2), \tag{3}$$

$$g_L \equiv 1 - \frac{\langle M^4 \rangle}{3 \langle M^2 \rangle^2} \tag{4}$$

Five values of the disorder (defined as the fraction of Mo sublattice sites occupied by Fe ions) have been considered: AS=0, 10%, 20%, 30%, and 40%.

III. RESULTS AND DISCUSSION

As a first result, it must be pointed out that the model used reproduces the dependence of the low-temperature saturation magnetization on the AS concentration found experimentally: $M_S = 4(1-2AS)\,\mu_B$/Fe ion.[14,16] As it is well known, this dependence is due to the AFM alignment of Fe ions in Mo sublattice due to the strong AFM coupling between n.n. Fe. The second direct consequence of the presence of AS is the systematic reduction of the Curie temperature. This is shown in Fig. 2(a) where the maximum of the different $\chi(T)$ curves shifts down in temperature when the fraction of AS is augmented. The same is observed for very low AS concentration (2% and 4%, not shown). From Fig. 2(a), it is also apparent that the value of the maximum of χ is also reduced when the amount of disorder is enhanced. In addition, the slope of χ^{-1} curves near T_C is enhanced with the fraction of AS. We attribute these effects to the strong AFM coupling between Fe-Fe n.n. pairs. First, as a result of this AFM coupling, the presence of AS promotes a reduction of the number of ions involved in the magnetic coupling: Fe in AS positions do not contribute to the enhancement of the fluctuations near T_C and the maximum of χ curves is reduced. Second, these Fe-Fe AFM pairs are also present above T_C reducing the effective paramagnetic moment, thus enhancing the slope of χ^{-1} curves. At high enough temperature [Fig. 2(b)] these correlations disappear and all the curves present the same slope. Indeed, this is the behavior observed by Tovar *et al.*[3] It follows that high-temperature measurements are crucial to avoid the contribution of AS when analyzing data in terms of a Curie-Weiss behavior.

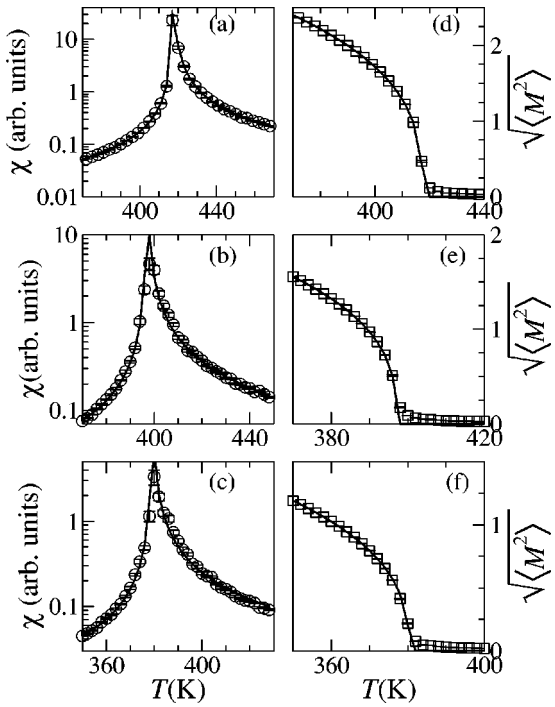

FIG. 3. χ [(a), (b), and (c) panels] and $\sqrt{\langle M^2 \rangle}$ [(d), (e), and (f) panels] obtained for $L=80$ with different amounts of disorder (a) and (d) AS=0; (b) and (e) AS=10%; (c), and (f) AS=20%. The solid lines are the best fits of the critical laws [Eqs. (5) and (6)].

Figure 3 shows the obtained susceptibility and magnetization (measured as $\langle M^2 \rangle^{1/2}$) for systems with size $L=80$ and different amounts of disorder. These curves have been successfully fitted (solid lines in Fig. 3) by the laws

$$\langle M^2 \rangle^{1/2} = \begin{cases} a \left(\dfrac{T_C - T}{T_C} \right)^{\beta} & \text{for } T \leqslant T_C \\ 0 & \text{for } T > T_C, \end{cases} \tag{5}$$

$$\chi = \begin{cases} a_1 \left(\dfrac{T_C - T}{T_C} \right)^{-\gamma} & \text{for } T < T_C \\ a_2 \left(\dfrac{T - T_C}{T_C} \right)^{-\gamma} & \text{for } T > T_C, \end{cases} \tag{6}$$

and used to obtain the critical exponents β and γ. The results extracted from these fits for different amounts of disorder and for sizes $L=40$ and 80 (for smaller sizes χ cannot be successfully adjusted with the same γ exponent at both sides of the transition) are reported in Table I. The values found in

TABLE I. Critical exponents and Curie temperatures obtained by fitting Eqs. (5) and (6) for different amounts of disorder and systems with sizes $L=40$ and 80.

	$L=40$				$L=80$			
	χ		$\sqrt{\langle M^2\rangle}$		χ		$\sqrt{\langle M^2\rangle}$	
AS	γ	T_C	β	T_C	γ	T_C	β	T_C
0	1.20(3)	417(2)	0.336(8)	417(2)	1.21(3)	417(2)	0.333(9)	417(2)
10%	1.12(3)	396(3)	0.35(1)	397(3)	1.11(3)	397(2)	0.35(2)	397(2)
20%	1.03(3)	380(2)	0.36(2)	379(2)	1.08(2)	379(2)	0.38(3)	380(2)
30%	0.95(4)	367(2)	0.37(3)	367(2)	1.00(2)	367(2)	0.38(3)	367(2)

the AS=0 case are compatible with those of Ising model $\gamma \simeq 1.25$ and $\beta \simeq 0.324$. It must be emphasized that these exponents are fairly comparable to experimental ones [$\gamma = 1.30(1)$ and $\beta = 0.389(4)$].[17]

Values of critical exponents and transition temperatures in Table I depend on the system size. In order to obtain these quantities in the thermodynamic limit we have used standard finite-size scaling techniques. This has been achieved by simulating systems with sizes $L=10$, 20, 30, 40, and 80 for the cases AS=0, 20%, and 40%. For each system size (and each AS concentration) we have first obtained the critical temperature [$T_C(L)$] from the inflexion point of $\langle M^2\rangle$. To do this we fitted a third-order polynomial to the critical region of these curves. According to standard finite-size scaling $T_C(L)$ must depend on L according to

$$T_C(L) = T_C(L\to\infty) + aL^{-1/\nu}, \tag{7}$$

where $T_C(L\to\infty)$ is the Curie temperature in the thermodynamic limit and ν is the critical exponent governing the divergence of the correlation length ($\xi \propto |T-T_C/T_C|^{-\nu}$). To obtain $T_C(L\to\infty)$ and a first estimation of ν we fit Eq. (7) to the values of $T_C(L)$ [Fig. 4(a)]. Afterward, we have done a regression of the power law $[T_C(L\to\infty)-T_C(L)] = aL^{-1/\nu}$ and obtained a second estimation of ν [Fig. 4(b)]. These two estimations are very similar and the differences between them have been considered as error bars of ν. The extracted values of T_C and ν are collected in Table II. We note that the exponent ν does not show a clear variation with AS. In principle, the same analysis could be done with the values of $T_C(L)$ obtained from the maximum of χ curves. However, the large error bar in $T_C(L)$ determined by this way prevented us from successfully performing this analysis.

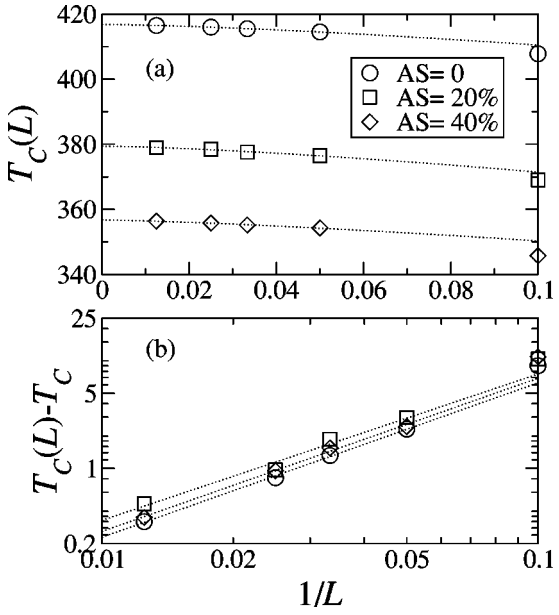

FIG. 4. (a) fit of Eq. (7) to the values of $T_C(L)$ obtained from the inflexion point of $\langle M^2\rangle^{1/2}$ curves. (b) Power law regression of $T_C - T_C(L)$ vs $1/L$, the slope is $1/\nu$.

Critical exponents β and γ have been obtained in the thermodynamic limit from the scaling expressions predicting that spontaneous magnetization (measured as $\langle M^2\rangle^{1/2}$) and the magnetic susceptibility for different system sizes must behave as

$$\langle M^2\rangle^{1/2} \propto L^{-\beta/\nu}\tilde{M}\left(L^{1/\nu}\frac{T-T_C}{T_C}\right), \tag{8}$$

$$\chi \propto L^{\gamma/\nu}\tilde{\chi}\left(L^{1/\nu}\frac{T-T_C}{T_C}\right). \tag{9}$$

Equation (8), applied at $T=T_C$, leads to $\langle M^2\rangle^{1/2}_{T=T_C} \propto L^{-\beta/\nu}$ and allows to obtain β exponents. The corresponding values are given in Table II and have been used to scale the spontaneous magnetization curves as shown in Figs. 5(a), 5(b) and 5(c). To obtain γ we have first plotted $\chi(\epsilon)$ (where $\epsilon = [(T-T_C)/T_C]L^{1/\nu}$) and we have integrated it in the interval $-3 \leqslant \epsilon \leqslant 3$. The value of this integral (I_L) must, according to Eq. (9), obey $I_L \propto L^{\gamma/\nu}$. The values obtained are included in Table II and have been used to scale the susceptibility curves as presented in Figs. 5(d), 5(e), and 5(f). The

TABLE II. Critical exponents and Curie temperatures obtained through finite-size scaling analysis.

AS	0	20%	40%
T_C (K)	416.8(4)	379.5(4)	356.8(6)
ν	0.70(6)	0.74(4)	0.70(8)
β	0.31(4)	0.37(2)	0.37(5)
γ	1.18(6)	1.48(4)	1.15(7)

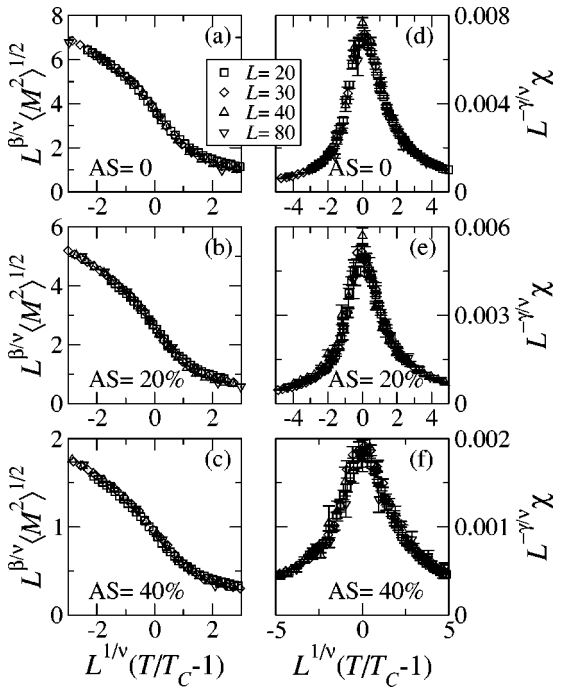

FIG. 5. Spontaneous magnetization [(a), (b), and (c)] and magnetic susceptibility [(d), (e), and (f)] scaled according to Eqs. (8) and (9) for different systems sizes and different concentrations of AS.

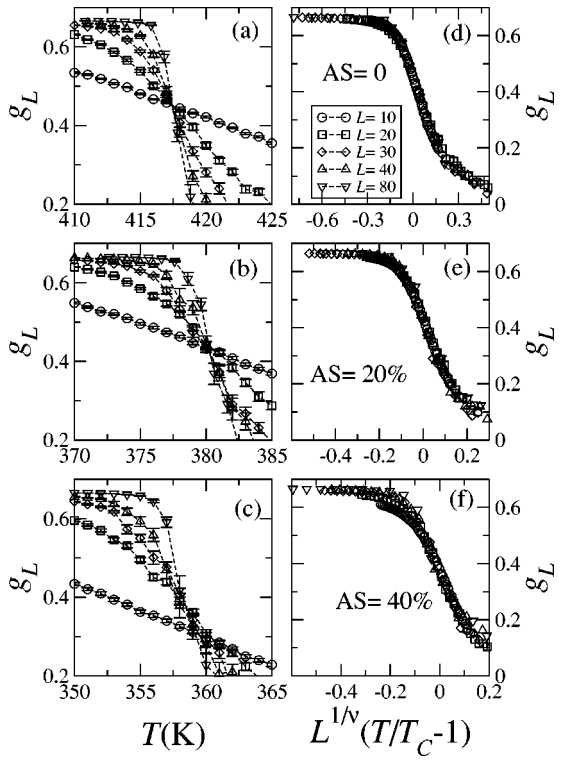

FIG. 6. (a), (b), and (c): Fourth-order Binder cumulant as a function of temperature for system sizes ranging between $L=10$ and 80. (d), (e), and (f): the same quantity scaled according to Eq. (10).

scaling of magnetization and susceptibility curves ensures that the values of critical exponents in Table II are, within the error bars, correct.

It appears from Fig. 5 that critical behavior is present up to a very high level of disorder (AS=40%). We have tried to corroborate this by studying the behavior of the fourth-order Binder's cumulant. This quantity is expected to present a unique crossing point when plotted as a function of temperature for different system sizes. This can be seen in Figs. 6(a) and 6(b) showing g_L for system sizes ranging in $10 \leqslant L \leqslant 80$ and for AS=0 and 20%. In contrast, for AS =40% [Fig. 6(c)], there are different crossing points for different system sizes. Fourth-order Binder's cumulant must scale according to the expression[18]

$$g_L \propto \tilde{g}\left(L^{1/\nu}\frac{T-T_C}{T_C}\right). \tag{10}$$

The matching on a single line is found for AS=0 and 20% [Figs. 6(d) and 6(e)] but not for AS=40% [Fig. 6(f)]. This can be interpreted as indicating the absence of a true phase transition for large AS concentration. However, it is also possible that the lack of accurate scaling to a single line is due to the relatively large errors in the simulations for this case.

It is of special interest to study the effect of the AS disorder on the shape of the magnetization curve. Experimentally, it is found that the presence of disorder widens the transition.[11] Figure 7 shows the comparison between scaled magnetization curves corresponding to AS=0 and AS =40% (with $L=80$). It can be appreciated that the transition is widened due to the presence of disorder. However, this broadening is less important than that found experimentally. This indicates that the origin of the experimentally observed widening of the magnetic transition cannot be attributed to AS effects in a homogeneous matrix but more likely, it reflects a certain distribution of AS defects from grain to grain. Such distribution of AS would introduce a distribution of Curie temperatures producing a broadening of the transition.

IV. CONCLUSIONS

We have formulated a spin model that takes into account the origin of the dominant magnetic interactions in Sr_2FeMoO_6 double perovskites. By means of Monte Carlo simulation we have studied it for different amounts of AS disorder. We have found that the model reproduces some of

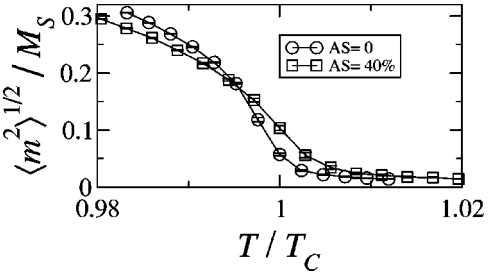

FIG. 7. Comparison of the transition widths for systems with AS=0 and AS=40%. The simulations correspond to systems with size $L=80$ and averages over 20 realizations.

the experimental results found in these compounds. In particular, the reduction of the saturation magnetization and the decrease of the susceptibility maximum when AS disorder is introduced. The behavior of the fourth-order Binder cumulant suggests that the criticality is lost at high enough AS concentration but a definitive answer to this point cannot be given.

We have found a systematic decrease of T_C with the amount of disorder. The experimental results reported for T_C depend somewhat on how T_C is determined, but T_C has been found to decrease with increasing AS.[11] This trend is reproduced by our model, although the dependence of T_C on AS found here is considerably stronger than that found experimentally. By contrast, some recent theoretical works predicted an enhancement of T_C at low concentrations of AS.[19] This has been attributed to the fact that the strong n.n. AFM interaction introduced by Fe in AS positions also FM aligns Fe in their neighborhood. We have found that this effect does not apply in our model because even at low concentrations of AS (2% and 4%) a monotonic lowering of T_C is obtained. It must be pointed out that, in our model, the magnetic interactions depend linearly on the number of Fe-Mo-Fe paths present. This linear relation will not apply if due to the presence of AS significant modification of the band structure occurs.

The experimentally observed broadening of the FM transition in double perovskites containing a large amount of AS is larger than that found by the simulations. This could be a consequence that in real systems there is a certain distribution of AS concentrations leading to a distribution of T_C. In addition, this distribution of AS concentration can contribute to the loss of criticality experimentally found at a large amount of disorder. Before closing we would like to stress that the simple model of magnetic interactions we have developed is a rigid model, where the strength of interactions is assumed to be constant, irrespectively of the presence of AS. It cannot be excluded that the subtle differences between experimental results and predictions reflect electronic rearrangements associated with the presence of defects. These issues, together with the study of the model under nonzero applied magnetic field, paying special attention to the comparison with the experimental Arrot's plots,[11] will be reported in the near future.

ACKNOWLEDGMENTS

We acknowledge Dr. E. Vives for fruitful discussions and a critical reading of the manuscript. We thank Grants Nos. MAT2002-03431 and MAT2003-07483-C02 CICyT, Spanish government, Advanced Magnetic Materials for a Responsive Engineering (UE), and Generalitat de Catalunya Grant No. 2001SGR-00334 projects for financial support. C.F. acknowledges financial support from MCyT (Spain). This research was done using computing resources of CESCA (DURSI, Generalitat de Catalunya, Fundació Catalana per a la Recerca and CICyT), we thank these institutions for the provision of CPU time.

[1] K.-I. Kobayashi, T. Kimura, H. Sawada, K. Terakura, and Y. Tokura, Nature (London) **395**, 677 (1998).
[2] S. Ray, A. Kumar, D.D. Sarma, R. Cimino, S. Turchini, S. Zennaro, and N. Zema, Phys. Rev. Lett. **87**, 097204 (2001).
[3] M. Tovar, M. Causa, A. Butera, J. Navarro, B. Martínez, J. Fontcuberta, and M. Passeggi, Phys. Rev. B **66**, 024409 (2002).
[4] D. Sánchez, J.A. Alonso, M. García-Hernández, M.J. Martínez-López, J.L. Martínez, and A. Mellergard, Phys. Rev. B **65**, 104426 (2002).
[5] J.A. Alonso, M.T. Casais, M.J. Martínez-Lope, J.L. Martínez, P. Velasco, A. Muñoz, and M.T. Fernández-Díaz, Chem. Mater. **12**, 161 (2000).
[6] B. García-Landa, C. Ritter, M.R. Ibarra, J. Blasco, P.A. Algarabel, R. Mahendiran, and J. García, Solid State Commun. **110**, 435 (1999).
[7] C. Ritter, M.R. Ibarra, L. Morellon, J. Blasco, J. García, and J. Teresa, J. Phys.: Condens. Matter **12**, 8295 (2000).
[8] J.M. Greneche, M. Venkatesan, R. Suryanarayanan, and J.M.D. Coey, Phys. Rev. B **63**, 174403 (2001).
[9] P. Algarabel, L. Morellon, J.D. Teresa, J. Blasco, J. García, M. Ibarra, T. Hernández, F. Plazaola, and J. Barandiarán, J. Magn. Magn. Mater. **226**, 1089 (2001).
[10] J. Navarro, L. Balcells, F. Sandiumenge, M. Bibes, A. Roig, B. Martínez, and J. Fontcuberta, J. Phys.: Condens. Matter **13**, 8481 (2001).
[11] J. Navarro, J. Nogués, J.S. Muñoz, and J. Fontcuberta, Phys. Rev. B **67**, 174416 (2003).
[12] J. Navarro, Ph.D. thesis, Universitat Autònoma de Barcelona, 2003.
[13] A. Aharony and E. Pytte, Phys. Rev. Lett. **45**, 1583 (1980).
[14] A. Ogale, S. Ogale, R. Ramesh, and T. Venkatesan, Appl. Phys. Lett. **75**, 537 (1999).
[15] O. Chmaissem, R. Kruk, B. Dabrowski, D. Brown, X. Xiong, S. Kolesnik, J. Jorgensen, and C. Kimball, Phys. Rev. B **62**, 14197 (2000).
[16] L. Balcells, J. Navarro, M. Bibes, A. Roig, B. Martínez, and J. Fontcuberta, Appl. Phys. Lett. **78**, 781 (2001).
[17] H. Yanagihara, W. Cheong, and M.B. Salamon, Phys. Rev. B **65**, 092411 (2002).
[18] K. Binder and D.W. Heermann, *Monte Carlo Simulation in Statistical Physics: an Introduction*, 3rd ed., Springer Series in Solid-State Sciences (Springer, New York, 1997).
[19] J. Alonso, L. Fernández, F. Guinea, F. Lesmes, and V. Martin-Mayor, Phys. Rev. B **67**, 214423 (2003).